Momentum and Heat Transfer in a Laminar Boundary Layer with Slip Flow

Michael J. Martin[*] and Iain D. Boyd[†]
University of Michigan, Ann Arbor, Michigan 48109-2104

Flow in a laminar boundary layer is modeled using a slip boundary condition. The slip condition changes the boundary layer structure from a self-similar profile to a two-dimensional structure. Although the slip condition generally leads to decreased overall drag, two-dimensional effects cause local increases in skin friction. Other effects include thinner boundary layers, delayed transition to turbulence, and changes in the heat transfer at the wall. Without a thermal jump condition, slip will lead to increased heat transfer. When a thermal jump boundary condition is added to simulate real gases, the heat transfer decreases to below the no-slip values.

Nomenclature

a	=	iteration coefficient
b	=	iteration coefficient
C_D	=	drag coefficient
c_p	=	specific heat ratio
F_D	=	drag force
f	=	nondimensional stream function
i	=	index in K_1 direction
j	=	index in η direction
K_1	=	nonequilibrium parameter
Kn	=	Knudsen number
L	=	length
Nu	=	Nusselt number
n	=	distance in tangential direction
P	=	static pressure
q''	=	heat flux
Re	=	Reynolds number
s	=	distance in normal direction
T	=	temperature
u	=	velocity in the x direction
v	=	velocity in the y direction
x	=	position in flow normal direction
y	=	position in flow tangential direction
α	=	thermal conductivity
β	=	slip length
γ	=	specific heat ratio
Δ	=	step size
δ	=	boundary layer thickness
δ^*	=	displacement thickness
η	=	nondimensional position
η_{99}	=	nondimensional boundary layer thickness
θ	=	momentum thickness
λ	=	mean free path
μ	=	viscosity
ρ	=	density
σ	=	accommodation coefficient
τ	=	shear stress
υ	=	kinematic viscosity

Subscripts

g	=	gas
L	=	length
M	=	momentum
o	=	freestream
slip	=	property of gas or liquid at wall
T	=	thermal
x	=	position on length of plate
δ	=	boundary layer thickness

Superscripts

$*$	=	nondimensional value
$'$	=	derivative with respect to η
$''$	=	second derivative with respect to η

I. Introduction

AS the number of applications of microelectromechanical systems (MEMS) increases, the study of gas and liquid flows at the microscale has become a topic of increasing interest [1,2]. In both gas and liquid phases, these flows are often dominated by surface interactions, making correct modeling of the wall boundary conditions essential. Slightly rarefied gas flows, with Knudsen numbers less than 0.1, are modeled using the Maxwell slip condition [3]:

$$u_{\text{slip}} = u_g - u_w = \lambda \frac{2 - \sigma_M}{\sigma_M} \frac{\partial u}{\partial n}\bigg|_{\text{wall}} + \frac{3}{4} \frac{\mu}{\rho T_g} \frac{\partial T}{\partial s}\bigg|_{\text{wall}} \quad (1)$$

where u_{slip} is the wall slip velocity, u_g is the gas velocity at the wall, u_w is the wall velocity, $\partial u / \partial n$ is velocity gradient normal to the wall, σ_M the tangential momentum accommodation coefficient, T_g is the temperature of the gas, and $\partial T / \partial s$ is the temperature gradient along the wall.

For an isothermal wall, this simplifies to

$$u^*_{\text{slip}} = Kn \frac{2 - \sigma_M}{\sigma_M} \frac{\partial u^*}{\partial n^*}\bigg|_{\text{wall}} \quad (2)$$

where Kn is the Knudsen number at the wall, u^* is the nondimensional velocity, and n^* is the nondimensional distance in the wall normal direction.

Recent research [4] suggests that as length scales in liquid flows approach the continuum limit, a similar slip condition may apply. This slip condition is given as

$$u_{\text{slip}} = \beta \frac{\partial u}{\partial n}\bigg|_{\text{wall}} \quad (3)$$

*Graduate Student Research Assistant, Department of Aerospace Engineering. AIAA Student Member.
†Professor, Department of Aerospace Engineering. AIAA Associate Fellow.

where β is the slip length for the liquid. Although experimental measurements [5] suggest that the slip length for hydrophobic surfaces with water are on the order of 1 μm, the existence of liquid slip, as well as the appropriate length scales for β, is still the subject of controversy within the fluid mechanics community [6].

A first-order solution, based on integral methods, of the boundary layer equations suggests that the boundary layer thins as a result of slip effects [7]. However, integral methods were unable to show any changes in skin friction. An expanded version of this analysis suggested that heat transfer was unaffected by the appearance of velocity slip [8]. Computational studies have also been made of external flow conditions, such as gas flows over flat plate airfoils [9]. These studies have shown that nonequilibrium effects will change the skin friction on a flat plate in slip flow.

This paper provides a semi-analytic solution to the boundary layer equations for a flat plate under slightly rarefied flow conditions. The changes to the flow structure, including velocity profile and boundary layer thickness, are analyzed. The changes in viscous drag and heat transfer for the flat plate are calculated and correlated as functions of flow properties.

II.   Fluid Flow in a Laminar Boundary Layer with Slip

A.   Formulation of Boundary Layer Equations with Slip Flow

As shown in Fig. 1, flow over a plate can be described as consisting of a uniform external flow region and a boundary layer of finite thickness.

The flow is governed by the continuity equation and conservation of momentum in the x direction:

$$\frac{\partial \rho}{\partial t} + \frac{\partial \rho u}{\partial x} + \frac{\partial \rho v}{\partial y} = 0 \qquad (4)$$

$$\frac{\partial u}{\partial t} + u\frac{\partial u}{\partial x} + v\frac{\partial u}{\partial y} = -\frac{\partial P}{\partial x} + \upsilon\left[\frac{\partial^2 u}{\partial x^2} + \frac{\partial^2 u}{\partial y^2}\right] \qquad (5)$$

This flow was first studied extensively by Blasius [10] who assumed steady, incompressible, laminar flow, no significant gradients of pressure in the x direction, and that velocity gradients in the x direction are small compared to velocity gradients in the y direction. Based on these assumptions, Eqs, (4) and (5) then simplify into the boundary layer equations given as

$$\frac{\partial u}{\partial x} + \frac{\partial v}{\partial y} = 0 \qquad (6)$$

$$u\frac{\partial u}{\partial x} + v\frac{\partial u}{\partial y} = \upsilon\frac{\partial^2 u}{\partial y^2} \qquad (7)$$

These equations can then be transformed, using the non-dimensionalizations and nondimensional stream functions given as
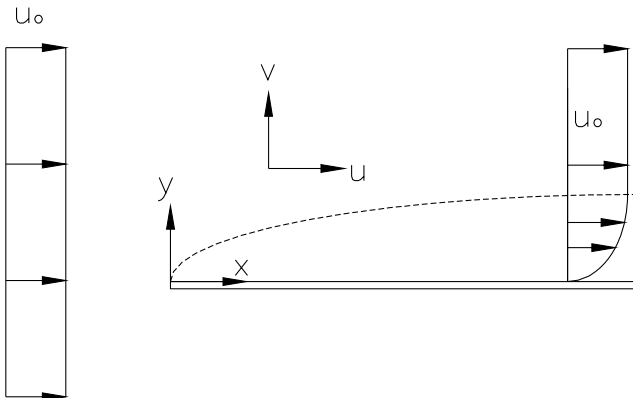

U₀

Fig. 1   Boundary layer flow over a flat plate.

$$x^* = x/L \qquad (8)$$

$$y^* = \frac{y}{(\upsilon L/u_o)^{1/2}} \qquad (9)$$

$$u^* = u/u_o \qquad (10)$$

$$v^* = \frac{v}{(\upsilon u_o/x)^{1/2}} \qquad (11)$$

$$\eta = \frac{y^*}{(x^*)^{1/2}} = \frac{y/(\upsilon L/u_o)^{1/2}}{(x/L)^{1/2}} = \frac{y}{(\upsilon x/u_o)^{1/2}} \qquad (12)$$

$$u^* = \frac{u}{u_o} = f'(\eta) \qquad (13)$$

$$v^* = \frac{v}{(\upsilon u_o/x)^{1/2}} = 0.5[\eta f'(\eta) - f(\eta)] \qquad (14)$$

where L is the length of the flat plate.

A governing equation for f can be found by substituting these results into the x momentum Eq. (7):

$$f'''(\eta) = -0.5f(\eta)f''(\eta) \qquad (15)$$

For flow at nonrarefied length scales, the boundary conditions for the problem are no slip, and no through flow at the wall, and u is equal to the freestream velocity as y approaches infinity. In nondimensional variables, these become

$$u^*(y=0) = 0 \Rightarrow f'(\eta=0) = 0 \qquad (16)$$

$$v^*(y=0) = 0 \Rightarrow f(\eta=0) = 0 \qquad (17)$$

$$u^*(y\to\infty) = 1 \Rightarrow f'(\eta\to\infty) = 1 \qquad (18)$$

Based on these boundary conditions, Blasius was able to solve the problem using a shooting method, which gave an initial value of

$$f''(\eta=0) = 0.33206 \qquad (19)$$

Using this result, Blasius calculated the self-similar laminar boundary layer, with a velocity profile and nondimensional shear stress.

When gas flow approaches the continuum limit, the no-slip condition given by Eq. (16) is replaced by the slip-flow condition given as Eq. (2). If we use the nondimensionalizations given in Eqs. (8–14), this condition can be nondimensionalized to obtain

$$f'(0) = \frac{(2-\sigma_M)}{\sigma_M} Kn_x Re_x^{1/2} f''(0) = K_1 f''(0) \qquad (20)$$

where Kn_x and Re_x are the Knudsen and Reynolds numbers based on x, and K_1 is a nondimensional parameter that describes the behavior at the surface:

$$K_1 = \frac{(2-\sigma_M)}{\sigma_M} Kn_x Re_x^{1/2} \qquad (21)$$

When liquid flows approach the continuum limit, an alternate definition of K_1 based on the slip length can be derived using the same nondimensionalizations:

$$K_1 = \frac{\beta}{x} Re_x^{1/2} \qquad (22)$$

The revised boundary condition suggests that self-similarity will be lost, and the velocity will be a function of both η and K_1. Although the definition of u^* is unchanged, the definition of v^* must be

modified to incorporate the derivative of the stream function with respect to K_1:

$$v^* = \frac{v}{(vuo/x)^{1/2}} = \frac{1}{2}\left[\eta\frac{\partial f(\eta, K_1)}{\partial \eta} - f(\eta, K_1) + K_1\frac{\partial f(\eta, K_1)}{\partial K_1}\right]$$

(23)

When all other derivatives in x are rewritten to include a K_1 term, the ordinary differential equation given in Eq. (15) is replaced by a partial differential equation:

$$\frac{\partial^3 f}{\partial \eta^3} = -0.5f\frac{\partial^2 f}{\partial \eta^2} - 0.5K_1\frac{\partial}{\partial \eta}\left[\frac{\partial f}{\partial \eta}\frac{\partial f}{\partial K_1}\right]$$

(24)

The no-slip governing equation will be recovered when K_1 is equal to zero. At large values of K_1, Eq. (24) faces three distinct problems: the emergence of a singularity, the breakdown of the boundary layer assumptions, and the breakdown of the Navier–Stokes equations. Each of these phenomena should be considered in greater depth.

Large values of K_1 correspond to small values of x, or the leading edge of the plate. Because the definition of η given in Eq. (12) is inversely proportion to the square root of x, the boundary layer equations approach a singularity as x approaches zero, corresponding to K_1 approaching infinity.

Even before nondimensionaliziation, Eq. (7) is not accurate at the leading edge of the plate. The boundary layer equations are formulated on the assumption that the velocity gradients in the x direction are small compared to velocity gradients in the y direction. At the leading edge of the plate, this assumption is no longer true, leading to formation of a Stokes flow region [11]. Correct use of the boundary layer equations requires that this region be relatively small, which requires a Reynolds number of 500 or greater.

For gas flows at values of K_1 that correspond to a Knudsen number of 0.1 or greater, the Navier–Stokes equations break down, and Eq. (24) is no longer an accurate physical description of the flow. However, this region is smaller than the Stokes flow region described above and can be disregarded so long as larger values of Reynolds numbers, and smaller values of K_1, are achieved downstream.

For all of these reasons, this formulation of the boundary layer equations is susceptible to error at large values of K_1. However, just as when the no-slip boundary layer is integrated, the error in the leading edge can often be disregarded. When the values are then integrated over x to provide quantities such as drag and heat transfer on the body, the contribution of the free-molecular and transition regions, and the error that is introduced in these areas, will be relatively small compared to the total integral.

To solve in the slip domain, the partial differential equation must be solved over large regions of K_1, including the entire slip-flow region, as well as into the transitional and free-molecular flow regions. This can be accomplished using a marching code, beginning from large values of K_1, and marching the code until K_1 approaches zero. Because large values of K_1 correspond to small values of x, this approach marches in the flow direction, similar to existing boundary layer codes [11].

B.   Numerical Solution of Fluid Flow in Boundary Layer Equations with Slip Flow

Equation (24) is discretized using center-difference approximations for all derivatives with respect to η. To simplify the expression, f' is substituted for $\partial f/\partial \eta$:

$$f'_{i,j} = \frac{f_{i,j+1} - f_{i,j-1}}{2\Delta\eta} + O[(\Delta\eta)^2]$$

(25)

Equation (24) then becomes

$$\frac{\partial^2 f'}{\partial \eta^2} = -0.5f\frac{\partial f'}{\partial \eta} - 0.5K_1\frac{\partial}{\partial \eta}\left[f'\frac{\partial f}{\partial K_1}\right]$$

(26)

For the mixed derivative, a first-order upwind expression is used, as shown in Eq. (27):

$$\frac{\partial}{\partial \eta}\left[f'\frac{\partial f}{\partial K_1}\right]_{i,j} = \frac{1}{\Delta\eta}\frac{1}{\Delta K_1}[f'_{i,j}(f_{i,j} - f_{i-1,j}) - f'_{i,j-1}(f_{i,j-1} - f_{i-1,j-1})]$$

(27)

This yields the following expression for $f_{i-1,j}$:

$$f_{i-1,j} = f_{i,j} + \frac{f'_{i,j-1}}{f'_{i,j}}(f_{i-1,j-1} - f_{i,j-1})$$
$$+ \frac{2\Delta K_1}{K_1 f'_{i,j}}\left(\frac{f'_{i,j+1} - 2.0f'_{i,j} + f'_{i,j-1}}{\Delta\eta} + \frac{f_{i,j}}{4.0}(f'_{i,j+1} - f'_{i,j-1})\right)$$

(28)

When K_1 is large, flow is uniform in the x direction, giving the initial conditions:

$$f'(K_1 \rightarrow \infty) = 1$$

(29)

$$f(K_1 \rightarrow \infty) = \eta$$

(30)

Along the wall, the boundary conditions are the no-through-flow condition given by Eq. (17) and the slip condition given by Eq. (20). The slip condition is implemented through the following first-order approximation:

$$f'_{i,1} = \frac{K_{1i}f'_{i,2}}{(K_{1i} + \Delta\eta_{\text{wall}})} + O\left(\frac{(\Delta\eta)^2}{(\Delta\eta + K_{1i})}\right)\frac{\partial^2 f'}{\partial \eta^2}$$

(31)

The proposed scheme is conditionally stable. The following stability criteria apply:

$$\Delta K_1 \leq \frac{7(\Delta\eta)^2 K_1}{3}$$

(32)

$$\Delta K_1 \leq \frac{(1 + f'_{i,j})\Delta\eta K_1}{2f_{i,j}}$$

(33)

From the initial conditions at large K_1 specified in Eqs. (29) and (30), a maximum step size ΔK_1 is calculated using Eqs. (32) and (33). The stream function at the next step is calculated explicitly using Eq. (28), and values of f' calculated using Eq. (25). Because the maximum step size ΔK_1 becomes prohibitively small as K_1 approaches zero, the calculation is halted when it reaches a value of K_1 of less than 0.005. The solution at K_1 equal to zero is then calculated using the classical no-slip solution.

Because this is an explicit marching scheme, there are no convergence criteria. Instead, the calculation is repeated with varying grid sizes to ensure grid independence. This algorithm is used with a starting K_1 value ranging from 100 to 200, and $\Delta\eta$ varying from 0.0001 to 0.005, to produce the results given.

C.   Computational Results for Fluid Flow

The value of the stream function f for K_1 ranging from 0 to 10, which includes the entire slip-flow region, is show in Fig. 2. This figure shows that, for any value of η in the boundary layer, f decreases as the flow becomes more rarefied. Values of u^* and v^* are shown in Figs. 3 and 4. These results show that, at any given vertical position η in the boundary layer, u^* will increase, and v^* will decrease, as the flow becomes more rarefied.

The nondimensional friction, or $f''(0)$, is shown in Fig. 5. Figure 5 shows the surprising result that the friction in the flow peaks not at the no-slip condition, but at a value of K_1 of approximately 0.50. This is a result of the loss of self-similarity in the flow.

Closer inspection of the velocity contours shows that the y velocity v^* also peaks locally for values of K_1 less than 1.0. This gives some insight into the reason for this local increase in friction. As the flow proceeds along the plate, the value of K_1 decreases, and the slip
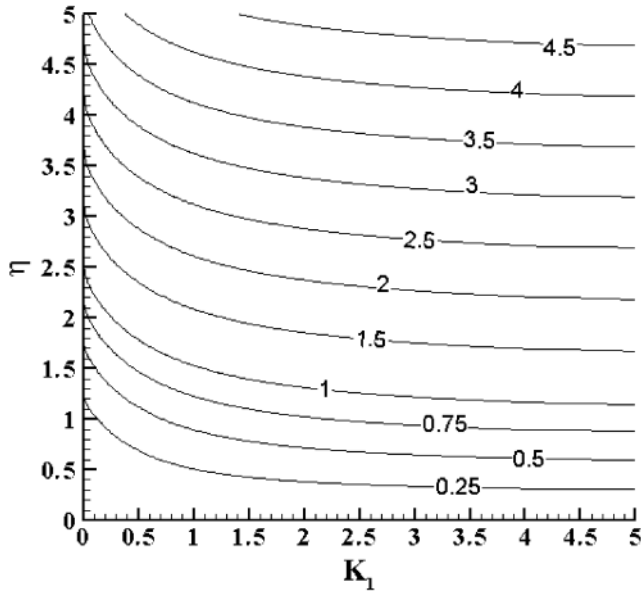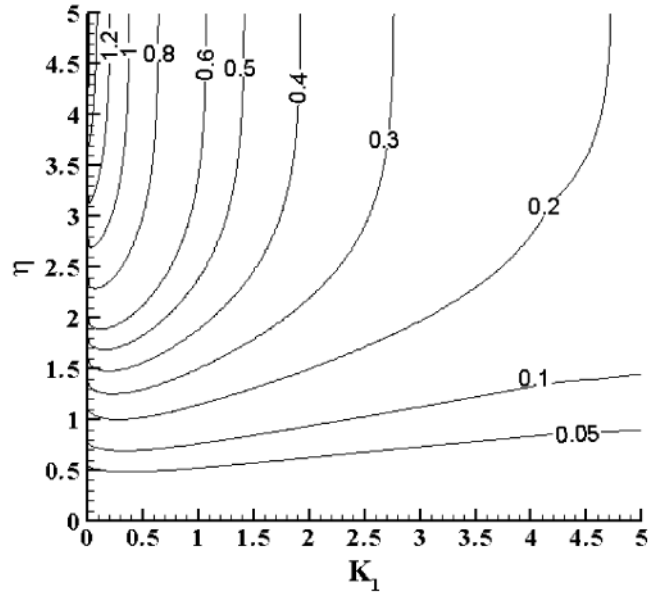
Fig. 2 Stream function as a function of position.

Fig. 4 Nondimensional y velocity as a function of position.
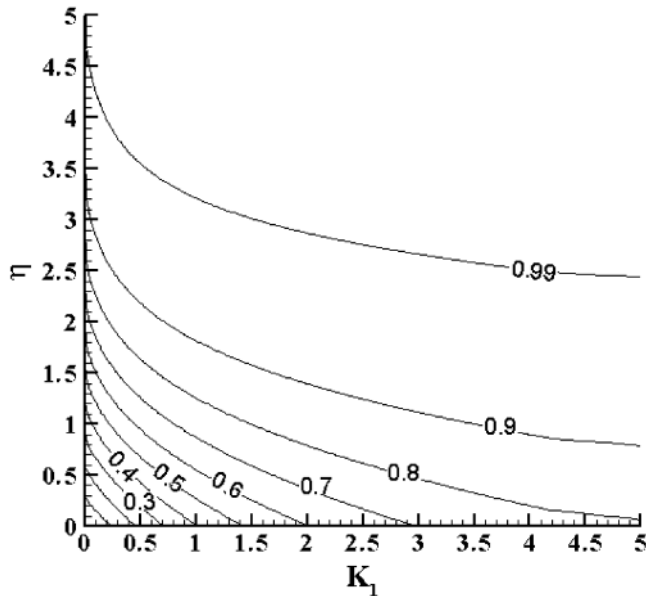
Fig. 3 Nondimensional x velocity as a function of position.
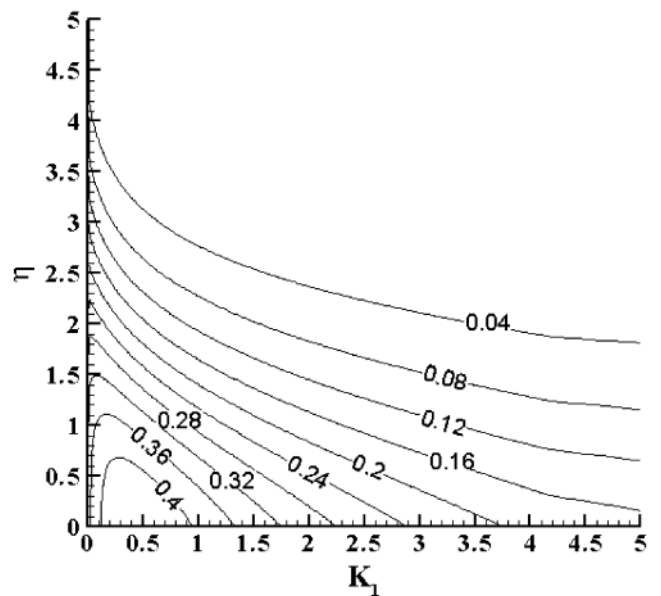
Fig. 5 Nondimensional friction as a function of position.

velocity along the wall also decreases. Continuity requires that fluid moves away from the wall, leading to an increase in v^*.

The nondimensional wall shear stress $f''(0)$ is shown in Fig. 6. $f''(0)$ has a peak value of 0.4358 when K_1 is equal to 0.0467. The two-dimensional effects cause a peak local friction of approximately 25% greater than the no-slip value. $f''(0)$ returns to the no-slip value as K_1 approaches 0 and asymptotically approaches zero as K_1 approaches infinity.

Figure 7 shows $f'(0)$, or the nondimensional slip velocity, as a function of K_1. These results show that the wall velocity asymptotically approaches the freestream velocity as rarefaction increases.

As the Knudsen number approaches zero, K_1 also approaches zero, where the no-slip condition and the classical boundary layer solution are recovered. As the Knudsen number becomes large, K_1 approaches infinity, and the nondimensional slip velocity approaches 1, indicating 100% slip at the wall.

Figure 8 shows the normalized x velocity profiles in the boundary layer for various values of K_1. One result that can be seen in Fig. 8 is that even as the wall velocity changes drastically, the overall

boundary layer thickness does not change as rapidly. The physical thickness of the boundary layer is given by Eq. (34):

$$\delta_{99} = \eta_{99} \, Re_x^{1/2} x \qquad (34)$$

For the no-slip boundary layer, η_{99} is a constant with a value of 5.0. For a boundary layer with slip, η_{99} varies along the plate. Figure 9 shows the value of η_{99}, where u^* is equal to 0.99, as a function of K_1. As the nondimensional wall slip velocity increases to greater than 0.99, the boundary layer thickness becomes zero. This occurs at values of K_1 greater than 80.

The definition of boundary layer thickness can be substituted into the definition of K_1:

$$K_1 = \frac{(2-\sigma)}{\sigma} \frac{Kn_\delta}{\eta_{99}} \qquad (35)$$

Because η_{99} does not change by large amounts over the plate, this result suggests that slip-flow effects are a strong function of boundary layer thickness.
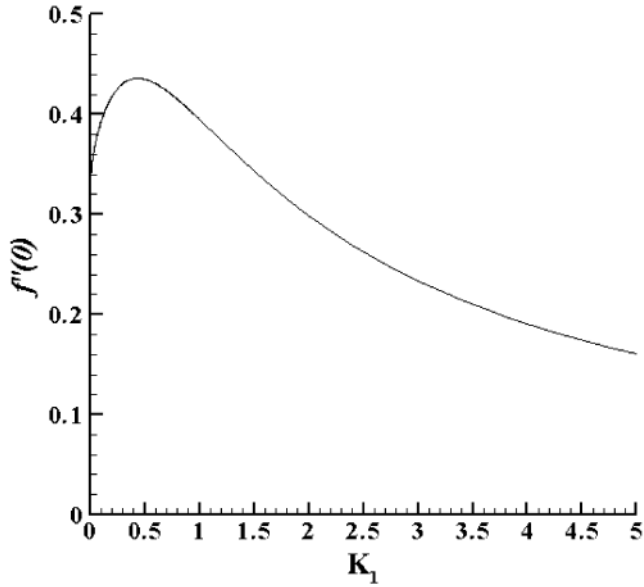
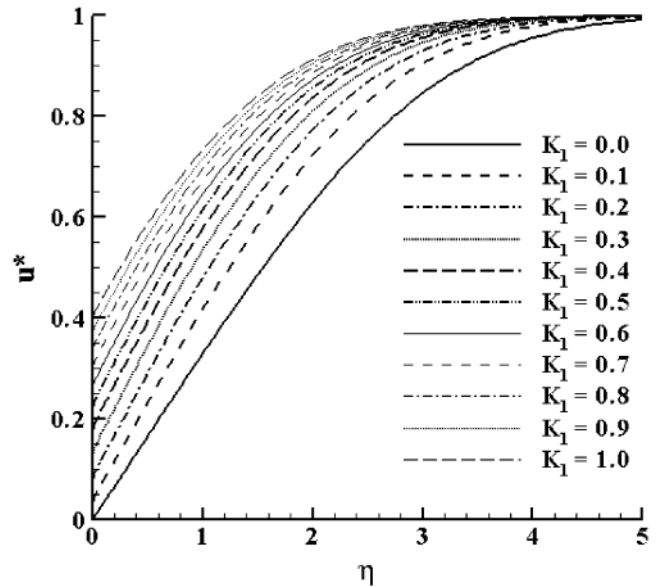**Fig. 6 Skin friction as a function of nonequilibrium.**

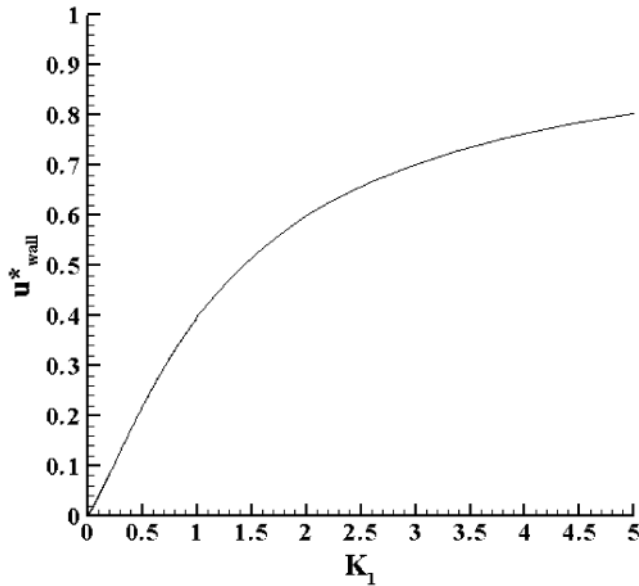**Fig. 8 Nondimensional x velocity profiles.**

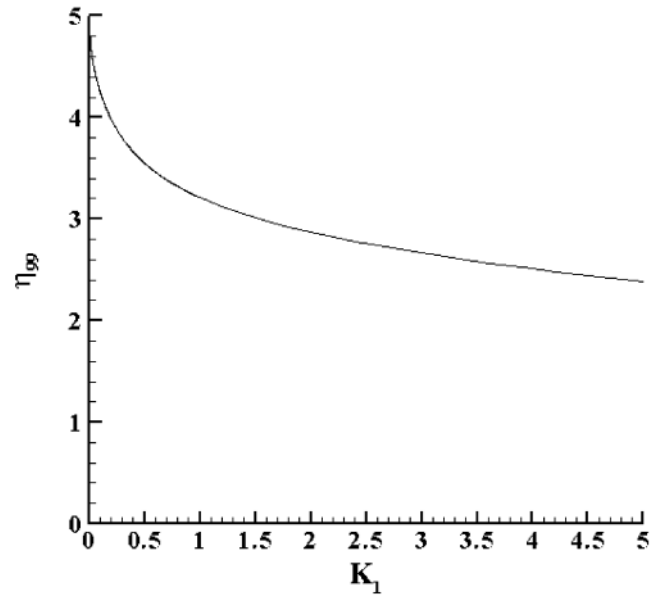**Fig. 7 Slip velocity as a function of nonequilibrium.**

Fig. 9 Boundary layer thickness as a function of nonequilibrium.

The displacement thickness and momentum thickness of the boundary layer will also vary with K_1. The displacement thickness, which measures the amount of the fluid displaced from the boundary layer, is defined as

$$\delta^* = \int_o^\infty \left(1 - \frac{u}{u_o}\right) dy \qquad (36)$$

This can be converted into nondimensional coordinates:

$$\frac{\delta^*}{\sqrt{u_o \upsilon / x}} = \int_o^\infty (1 - f') \, d\eta \qquad (37)$$

The momentum thickness, which measures the amount of momentum removed from the boundary layer, is defined as

$$\theta = \int_o^\infty \frac{u}{u_o}\left(1 - \frac{u}{u_o}\right) dy \qquad (38)$$

This can be expressed in nondimensional form:

$$\frac{\theta}{\sqrt{u_o \upsilon / x}} = \int_o^\infty f'(1 - f') \, d\eta \qquad (39)$$

The nondimensional momentum thickness and displacement thickness as functions of K_1 are plotted in Fig. 10. These results show that both the velocity and momentum thickness decrease as K_1, and the amount of slip, increase. The results of this analysis can also be used to predict possible transition to turbulence within a rarefied boundary layer. A Reynolds number based on velocity thickness is calculated, as shown in Eq. (40):

$$Re_\delta = \frac{\rho \bar{u} \delta^*}{\mu} \qquad (40)$$

Previous researchers have found that laminar boundary layers become unstable when Re_δ approaches 520 [12]. of slip is to decrease δ^*, this suggests that transition to turbulence may be delayed in a rarefied boundary layer.
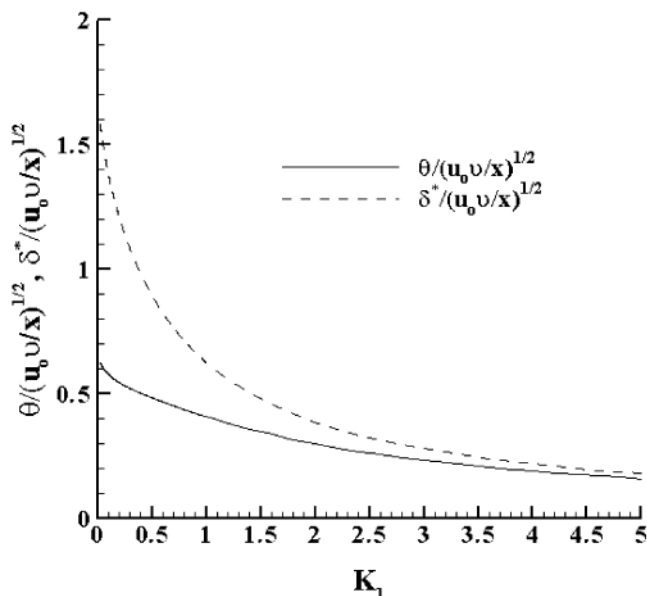
Fig. 10 Velocity and momentum thickness as functions of non-equilibrium.

Fig. 11 Drag coefficient as a function of nonequilibrium.

D. Calculation of Drag Force

There are two engineering reasons to be interested in slip flow over a flat plate: decreases in skin friction and changes in heat transfer along the surface.

The wall friction τ_w for a laminar boundary layer is given by the expression below:

$$\tau_w = \mu\left(\frac{\partial v}{\partial x} + \frac{\partial u}{\partial y}\right) = \mu\frac{\partial u}{\partial y} = \frac{\rho^{1/2}\mu^{1/2}u_o^{3/2}}{x^{1/2}}f''(0) \qquad (41)$$

The friction is proportional to the value of $f''(0)$ given in Fig. 6. Equation (41) can be integrated over the entire plate to obtain the net viscous drag force:

$$F_D = \rho^{1/2}\mu^{1/2}u_o^{3/2}\int_0^L \frac{f''(0)}{x^{1/2}}\,dx \qquad (42)$$

The drag coefficient C_D is defined as

$$C_D = \frac{F_D}{L(\rho U^2/2)} \qquad (43)$$

where F_D is the drag per unit span of the airfoil.

For a flat plate with no slip, the drag coefficient can be obtained by integrating analytically, to obtain

$$C_D = 1.328\, Re_L^{-1/2} \qquad (44)$$

For a flat plate with slip, the result must be obtained numerically. By substituting the definition of K_1 into (42), and performing the appropriate change of variables, we obtain

$$C_D = 4.0Re_L^{-1/2}K_1\int_{K_1(L)}^{\infty} \frac{f''(0)}{K_1^2}\,dK_1 \qquad (45)$$

The drag coefficient based on this integral is plotted in Fig. 11. The percent change in drag due to these effects compared to the no-slip solution is plotted in Fig. 12. These results show a slight increase in drag for slightly rarefied flows and then a large decrease in drag at higher Knudsen numbers.
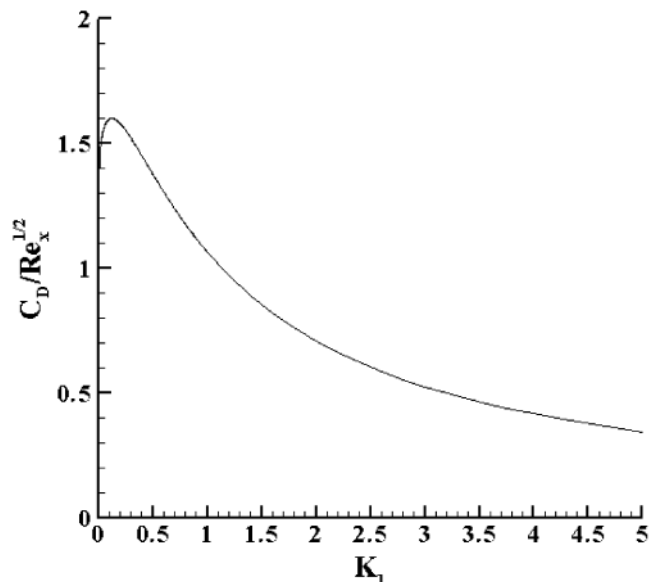
III. Heat Transfer in a Laminar Boundary Layer with Slip

A. Formulation of Boundary Layer Heat Transfer Equations with Slip Flow

Once the velocity profile is calculated, the heat transfer in a slip flow can be calculated using the same approach that is used in the nonslip solution [13]. If viscous dissipation is neglected, then the equation for conservation of energy in a boundary layer with steady flow is given as

$$u\frac{\partial T}{\partial x} + v\frac{\partial T}{\partial y} = \frac{\alpha}{\rho c_p}\frac{\partial^2 T}{\partial y^2} \qquad (46)$$

A nondimensional temperature T^* can be defined using the stream temperature T_o and the surface temperature T_w:

$$T^* = \frac{T - T_w}{T_o - T_w} \qquad (47)$$

If we assume that T^* is a function of η and K_1, and apply the appropriate nondimensionalizations, Eq. (47) can be rewritten as
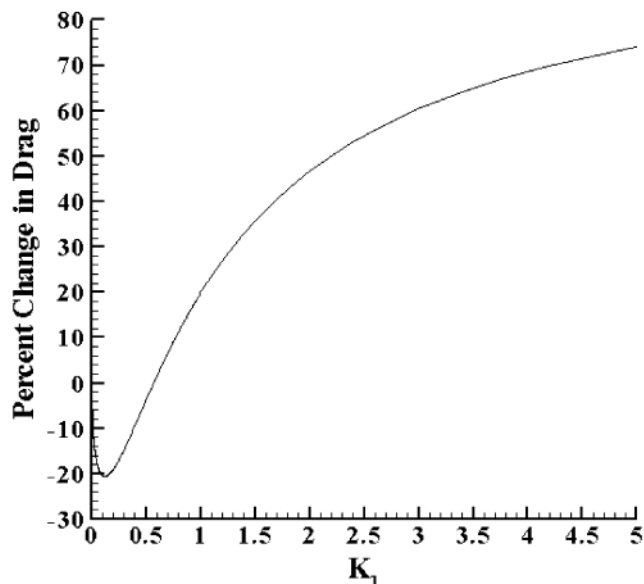

Fig. 12 Change in drag coefficient as a function of nonequilibrium.

$$0 = \frac{\partial^2 T^*}{\partial \eta^2} + Pr\left[\left(\frac{\eta u^*}{2} - v^*\right)\frac{\partial T^*}{\partial \eta} + K_1 u^* \frac{\partial T^*}{\partial K_1}\right] \quad (48)$$

where Pr is the Prandtl number of the fluid.

The heat transfer equations are discretized using center-difference approximations in the η direction, and a forward difference approximation in the K_1 direction, similar to the method used to solve the momentum equation. This results in the expression:

$$T^*_{i-1,j} = [a+b]T^*_{i,j+1} + [1-2.0a]T^*_{i,j} + [a+b]T^*_{i,j-1} \quad (49)$$

where

$$a = \frac{\Delta K_1}{Pr u^* K_1 (\Delta \eta)^2} \quad (50)$$

and

$$b = \frac{\Delta K_1}{2u^* K_1 \Delta \eta}\left(\frac{\eta u^*}{2} - v^*\right) \quad (51)$$

The stability criterion requires that all coefficients remain positive:

$$\Delta K_1 \leq = \frac{Pr K_1 f'_{i,j}(\Delta \eta)^2}{4.0} \quad (52)$$

$$\Delta \eta \leq \frac{4.0 Pr}{f_{i,j}} \quad (53)$$

The correct solution of the boundary layer heat transfer will require use of appropriate wall boundary conditions. The thermal boundary conditions for slip flow of a gas will differ from those of slip flow of a liquid, and the two cases will be considered separately.

B. Heat Transfer with Slip Without a Temperature Jump

Thermal boundary conditions for liquids at the microscale have not been extensively studied. Currently, calculations for heat transfer in liquids at the microscale assume that there is no thermal jump accompanying the velocity jump. If this is correct, then for liquids the temperature boundary condition at the wall will be the same as for nonslip flows:

$$T(\eta = 0) = T_s \quad (54)$$

In nondimensional form, this becomes

$$T^*(\eta = 0) = 0 \quad (55)$$

The boundary condition far from the wall will be

$$T(\eta = \infty) = T_\infty \quad (56)$$

In nondimensional form, this becomes

$$T^*(\eta = \infty) = 1 \quad (57)$$

At large values of K_1, the velocity approaches uniform flow, and the steady-state energy equation becomes

$$\frac{\partial^2 T^*}{\partial \eta^2} + \frac{Pr}{2}\eta\frac{\partial T^*}{\partial \eta} = 0 \quad (58)$$

This equation can be solved as an ordinary differential equation. The solution to this equation is used as the boundary condition at large values of K_1:

$$T^*(K_1 \to \infty) = \mathrm{erf}[\sqrt{Pr}\eta/2] \quad (59)$$

Using these boundary conditions, the heat transfer of a liquid boundary layer with wall slip is computed for Prandtl numbers of 1.0, 2.0, 3.0, 4.0, and 5.0. These values represent typical values for water and organic solvents near room temperature.
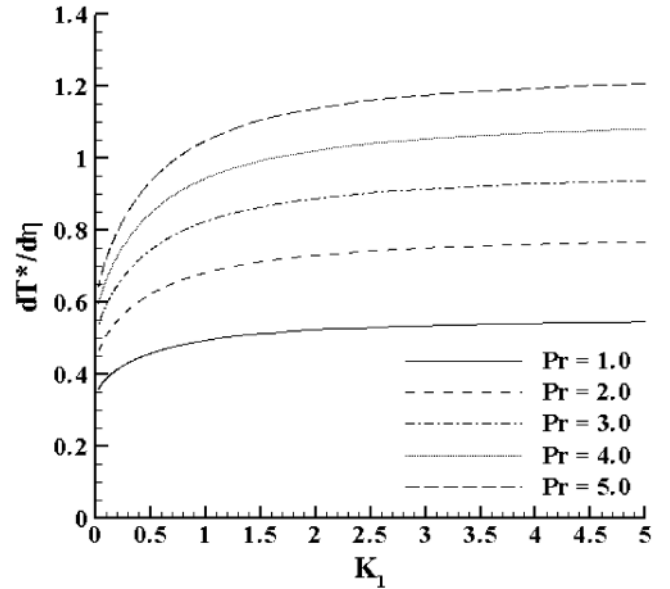

Fig. 13 Wall temperature gradient as a function of nonequilibrium for liquid flows.

The heat transfer coefficient h is proportional to the local derivative at the wall:

$$h = \frac{q''_s}{T_w - T_o} = -\frac{T_o - T_w}{T_w - T_o}\alpha\frac{\partial T^*}{\partial y}\Big|_{y=0} = \alpha\left(\frac{\rho u_o}{\mu x}\right)^{1/2}\frac{dT^*}{d\eta}\Big|_{\eta=0} \quad (60)$$

where q''_s is the surface heat flux.

The derivative of the temperature at the wall as a function of K_1 is shown in Fig. 13. For the no-slip condition, the derivative at the wall is approximated by the following:

$$\frac{dT^*}{d\eta}\Big|_{\eta=0} = 0.332 Pr^{1/3} \quad (61)$$

When compared with the no-slip results, Fig. 13 shows that for a liquid slip flow, the derivative at the wall, and the wall heat transfer, will increase as a result of slip.

To find the total heat transfer within the slip boundary layer, we integrate over the entire plate:

$$\bar{h} = \frac{1}{L}\int_o^L k\left(\frac{u_o}{\nu x}\right)^{1/2}\frac{dT^*(0)}{d\eta}\,dx \quad (62)$$

Substituting the definition of K_1 into Eq. (62) transforms the equation into:

$$\overline{Nu}_L = 2Re_L^{1/2}K_1\int_{K_1(L)}^\infty\frac{dT'(0)}{K_1^2}\,dK_1 \quad (63)$$

This equation is used to calculate the average heat transfer over the entire surface, as shown in Fig. 14. These results can be compared with the no-slip value for the Nusselt number:

$$\overline{Nu}_L = 0.664 Re_L^{1/2}Pr^{1/3} \quad (64)$$

Figure 14 shows the average heat transfer over a flat plate increases when slip occurs.

C. Heat Transfer in Gas Flows with Slip

The same rarefied flow effects that produce velocity slip at the surface for gas flows will also produce a temperature jump [3]. The temperature jump boundary condition is given as
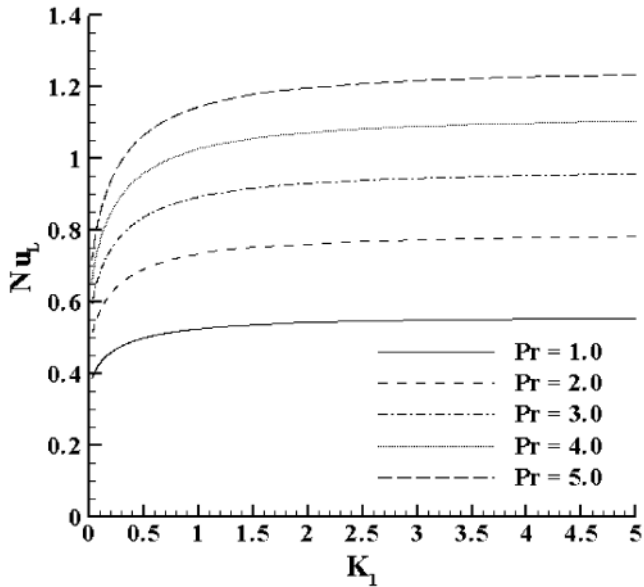
Fig. 14 Average Nusselt number as a function of nonequilibrium for liquid flows.

Fig. 16 Wall temperature as a function of nonequilibrium for $\gamma = 5/3$.

$$T_{\text{gas}} - T_{\text{wall}} = \frac{\lambda}{Pr} \frac{2 - \sigma_T}{\sigma_T} \frac{2\gamma}{\gamma + 1} \frac{\partial T}{\partial n}\bigg|_{\text{wall}} \qquad (65)$$

where σ_T is the thermal accommodation coefficient.

Equation (65) can be nondimensionalized to obtain

$$T^*(\eta = 0) = \frac{1}{Pr} \frac{2 - \sigma_T}{\sigma_T} \frac{2\gamma}{\gamma + 1} Kn_x Re_x^{1/2} \frac{\partial T^*}{\partial \eta}\bigg|_{\text{wall}} \qquad (66)$$

Data on thermal accommodation coefficients are extremely limited [14], but the thermal accommodation coefficient and the momentum accommodation coefficients appear to be approximately equal. If this assumption is used, then Eq. (66) simplifies to

$$T^*(\eta = 0) = \frac{1}{Pr} \frac{2\gamma}{\gamma + 1} K_1 \frac{\partial T^*}{\partial \eta}\bigg|_{\text{wall}} \qquad (67)$$

At large values of K_1, the temperature jump will become infinitely large, and the gradients at the wall will be negligible, giving a uniform temperature field:
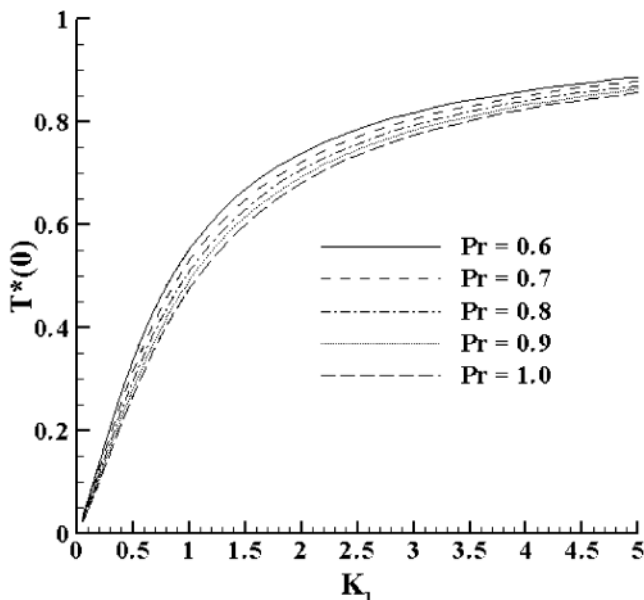
$$T^*(K_1 \to \infty) = 1 \qquad (68)$$

Figures 15 and 16 show the wall temperature as a function of K_1 and Pr for values of γ of 7/5 for a diatomic gas and 5/3 for a monatomic gas. These results show the temperature jump is a substantial percentage of the temperature difference for the flow in the slip-flow regime.

Figures 17 and 18 show the wall temperature derivative as a function of K_1 and Pr for values of γ of 7/5 and 5/3. These results show that the heat transfer increases with increased Prandtl number. The heat transfer also increases as the specific heat ratio decreases. However, this change is generally less than 1%. These results also show that the local heat transfer peaks at a value of K_1 of approximately 0.5. The peak location increases with increased Prandtl number and decreases with increased specific heat ratio.

When these results are compared with the no-slip results, it is clear that heat transfer at the wall will decrease in highly rarefied flows and increase under moderately rarefied conditions. For slightly rarefied flows, the increased velocity near the surface more than offsets the reduced heat transfer due to the temperature jump. For flows with
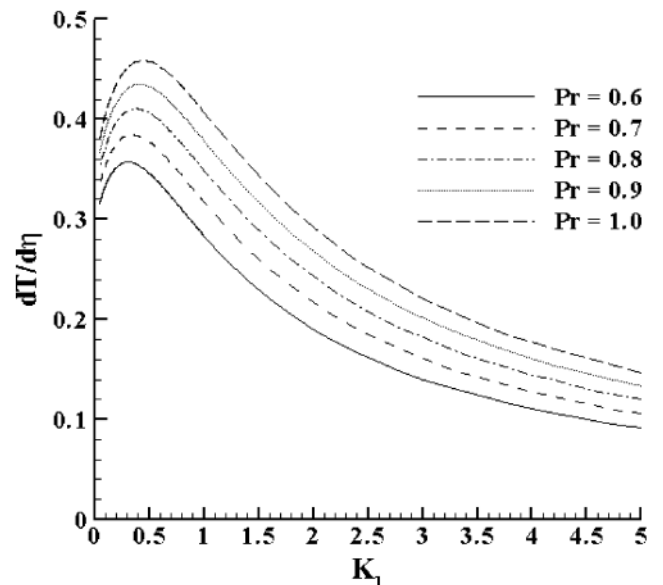

Fig. 15 Wall temperature as a function of nonequilibrium for $\gamma = 7/5$.

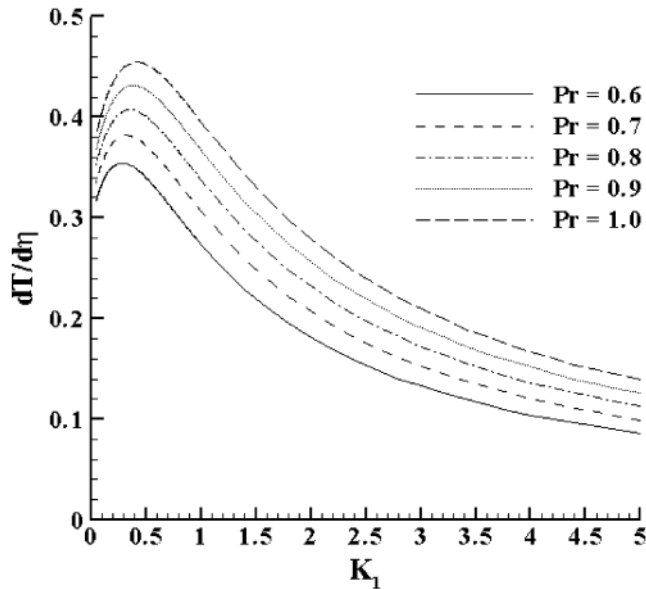Fig. 17 Wall temperature gradient as a function of nonequilibrium for $\gamma = 7/5$.

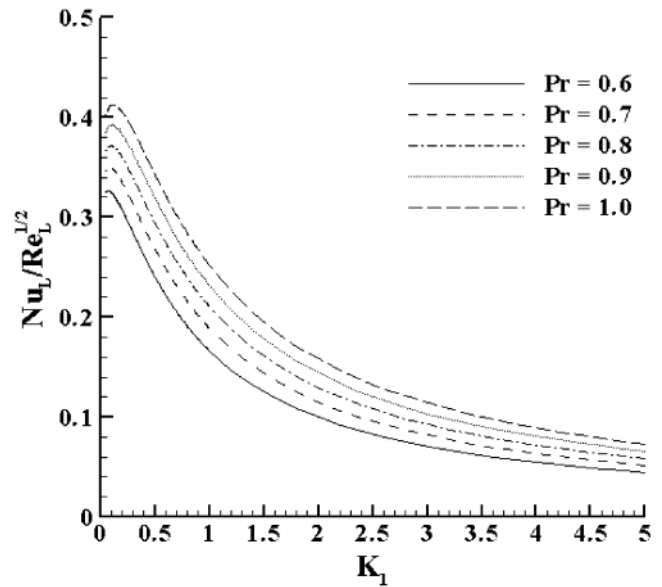**Fig. 18 Wall temperature gradient as a function of nonequilibrium for $\gamma = 5/3$.**

Fig. 20 Average Nusselt number as a function of nonequilibrium for $\gamma = 5/3$.
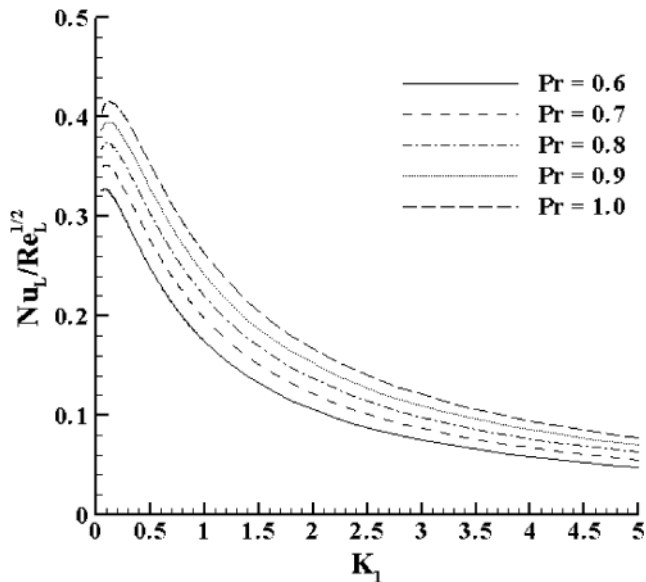

Fig. 19 Average Nusselt number as a function of nonequilibrium for $\gamma = 7/5$.

larger Knudsen numbers, the heat transfer result is dominated by the temperature jump condition. The decreased heat transfer at higher Knudsen numbers agrees qualitatively with experimental results for heat transfer in heated cylinders at these Knudsen numbers [15].

Figures 19 and 20 show the average Nusselt number as a function of K_1 and Pr for values of γ of $7/5$ and $5/3$. These results again show an increase in heat transfer under slightly rarefied conditions and a decrease in heat transfer under highly rarefied conditions.

IV. Conclusion

The equations for a laminar boundary layer can be solved nondimensionally in the presence of slip. The boundary layer loses the self-similarity of the no-slip Blasius solution. The loss of self-similarity leads to an increase in skin friction under some conditions. Other effects of slip included a thinner boundary layer and a more stable velocity profile.

The heat transfer in the boundary layer is also affected by the presence of slip. In liquid flows, where there is no temperature jump,

the heat transfer increases as the slip velocity increases. In gas flows, a temperature jump condition is added and shown to scale with the velocity slip. The presence of the thermal jump condition decreases the heat transfer in the system. For slightly rarefied flows, increased fluid velocity near the wall more than offsets effects of the temperature jump, and the heat transfer will still be greater than for the no-slip case. For more rarefied flows, the heat transfer will decrease to values less than those of the no-slip case.

These results can be applied to analyze a variety of systems, including potential microdevice designs and flight in low-density atmospheres.

References

[1] Ho, C. M., and Tai, Y. C., "Micro-Electro-Mechanical Systems (MEMS) and Fluid Flows," *Annual Review of Fluid Mechanics*, Vol. 30, 1998, pp. 579–612.

[2] Gad-el-Hak, M., "The Fluid Mechanics of Microdevices—The Freeman Scholar Lecture," *Journal of Fluids Engineering*, Vol. 121, No. 1, 1999, pp. 5–33.

[3] Maxwell, J. C., "On Stresses in Rarefied Gases Arising from Inequalities of Temperature," *Philosophical Transactions of the Royal Society of London*, Vol. 170, 1879, pp. 231–256.

[4] Wantanabe, K., Yanuar, and Mizunama, H., "Slip of Newtonian Fluids at Slid Boundary," *JSME International Journal (B)*, Vol. 41, No. 3, 1998, pp. 525–529.

[5] Tretheway, D. C., and Meinhart, C. D., "Apparent Fluid Slip at Hydrophobic Microchannel Walls," *Physics of Fluids*, Vol. 14, No. 3, 2002, pp. L9–L12.

[6] Stone, H. A., Stroock, A. D., and Ajdari, A., "Engineering Flows in Small Devices," *Annual Review of Fluid Mechanics*, Vol. 36, 2004, pp. 381–411.

[7] Lin, T. C., and Schaaf, S. A., "Effect of Slip on Flow Near a Stagnation Point and in a Boundary Layer," NACA TN 2568, 1951.

[8] Kogan, M. N., *Rarefied Gas Dynamics*, Plenum Press, New York, 1969, pp. 386–400.

[9] Sun, Q., and Boyd, I. D., "Flat-Plate Aerodynamics at Very Low Reynolds Number," *Journal of Fluid Mechanics*, Vol. 502, March 2004, pp. 199–206.

[10] Blasius, H., "Grenzschichten in Flüssigkeiten mit kleiner Reibung," *Zeitschrift für Mathematik und Physik*, Vol. 56, No. 1, 1908, pp. 1–37.

[11] White, F., *Viscous Fluid Flow*, 2nd ed., McGraw–Hill, New York, 1991, pp. 276–282.

[12] Schlichting, H., *Boundary Layer Theory*, 2nd ed., McGraw–Hill, New York, 1960, pp. 391–408.

[13] Incropera, F. P., *Introduction to Heat Transfer*, 3rd ed., Wiley, New York, 1990, pp. 386–399.

[14] Karniadakes, G. E., and Beskok, A., *Microflows*, Springer–Verlag, New York, 2002, pp. 51.

[15] Baldwin, L., Sandborn, V., and Laurence, J., "Heat Transfer from Transverse and Yawed Cylinders in Continuum, Slip, and Free Molecule Air Flows," *Journal of Heat Transfer*, Vol. 82, No. 2, 1960, pp. 77–88.